International Journal of Robotics and Control Systems
Vol. 5, No. 6, 2025, pp. 2808-2830
ISSN 2775-2658
http://pubs2.ascee.org/index.php/ijrcs

Robust Output Feedback Linearization Control of Nonlinear CSTR via the Grey Wolf Algorithm and Kharitonov-Based Stability

Yazen Hudhaifa Shakir Alnema [a,1,*], Abdullah Ibrahim Abdullah [a,2]

[a] Systems and Control Engineering, College of Electronics Ninevah University, Al-Jawsaq, Mosul 41002, Iraq
[1] yazen.shakir@uoninevah.edu.iq; [2] abdullah.abdullah@uoninevah.edu.iq
[*] Corresponding Author

ARTICLE INFO

Article history
Received August 04, 2025
Revised October 29, 2025
Accepted December 02, 2025

Keywords
CSTR;
High-Gain Observer;
Feedback Linearization;
Grey Wolf Optimizer;
Robust Nonlinear Control;
Kharitonov Theorem;
Process Control

ABSTRACT

This academic paper develops a novel combination of multiple control design techniques to generate a robust nonlinear control strategy for a Continuous Stirred Tank Reactor (CSTR). The core challenge is maintaining optimal performance when essential parameters such as reaction kinetics and heat transfer coefficients are unknown but bound. The main contribution is the synergistic use of a Grey Wolf Optimizer (GWO) to concurrently tune the gains of both a High-Gain Observer (HGO) and a feedback linearization controller, realizing a balanced and high-performance system. The methodology combines HGO-based state estimation with a feedback linearization controller. Furthermore, Kharitonov's theorem formally guarantees closed-loop stability under parametric uncertainties. The proposed controller was validated through simulations conducted under realistic operating conditions, proving its ability to robustly track temperature setpoints with faster settling time and smaller overshoot, even in the presence of variations in system parameters and external disturbances. In conclusion, this work establishes a systematic framework for employing advanced control theories to increase the efficiency and stability of a nonlinear CSTR plant.

1. Introduction

1.1. CSTR Control in General

The Continuous Stirred Tank Reactor (CSTR) is a cornerstone of the chemical processing industry, essential for manufacturing a vast range of products. However, the dynamics are inherently nonlinear in addition to the complex heat and mass transfer phenomena, and susceptibility to parametric uncertainties presents significant control challenges [1]. The primary objective required in CSTR control is to maintain the reactor's temperature and product concentration as desired to ensure safety, efficiency, and quality product. A key difficulty arises from the fact that the CSTR's equilibrium point is often not at the origin, complicating the design of globally stable control systems [1], [2]. Furthermore, critical parameters such as reaction kinetics and heat transfer coefficients are frequently unknown or time-varying, making traditional linear control methods inadequate [3], [4].

Thus, the development of robust, high-performance nonlinear control strategies still an active and critical area of research.

1.2. Development of Control Techniques for CSTRs

1.2.1. Traditional Approaches and Its Limitations

From the past to the present, Proportional-Integral-Derivative (PID) controllers have been the mainstay of industrial process control due to their simplicity and effectiveness in linear or near-linear operating regimes. Though their performance was significantly depicted when applied to the highly nonlinear dynamics of CSTRs, they often did not succeed in providing robust stability across a wide range of operating conditions [3]. Recently, researchers' attentions have been paid to optimizing PID controllers using advanced techniques. For example, metaheuristic algorithms such as the firefly algorithm (FA) [5] and enhanced Particle Swarm Optimization (PSO) [6] have been used as PID parameters tuner, showing improved performance. Ajlouni et al. [3] proposed a hybrid machine learning-metaheuristic approach to increase PID robustness in CSTRs. Despite these improvements, the linear nature of PID controllers remains a limitation when dealing with strong nonlinearities and uncertainties; in other words, they satisfy local stability, not global. Fuzzy logic controllers (FLCs), compared with PIDs, are more flexible and offer an alternative by incorporating heuristic knowledge into the control law. They have been successfully applied to various processes, including motion control [7] and electric drives [8]. Nevertheless, FLCs cannot ensure the stability in a formal manner , which is a major concern for safety-critical chemical processes [9], [10]. Similarly, adaptive control techniques show promise by adjusting controller parameters online to handle with system uncertainties [48]. Yet, as noted by Wen et al. [11] and Jiang et al. [12], they can suffer from slow convergence and potential instability when applied to complex nonlinear systems without careful design.

1.2.2. Advanced Nonlinear Control Strategies

To overcome the limitations of traditional methods, research has shifted towards advanced nonlinear control strategies. Transforming a nonlinear system model into an equivalent linear one is a technique that is algebraically achieved via the powerful feedback linearization approach, allowing the application of well-established linear control theory [13], [14]. This method has been successfully applied to CSTRs [15] and other complex systems such as unmanned aerial vehicles, known shortly as UAVs [16]. One of the main drawbacks of the feedback linearization technique is that accurate information is required about the model of the system and full state variables must be available, which is often not practical in real-world applications.

1.3. State Estimation

1.3.1. High-Gain Observers (HGOs)

The full state information should be addressable, the role of state observers are employed to estimate unmeasured variables. High-Gain Observers (HGOs) have emerged as a powerful tool for a broad class of nonlinear systems [17], [18]. The core principle of HGOs is the use of a high gain parameter to ensure fast convergence of the estimated states to the true states. HGOs have found applications in diverse fields, from micro-robotics [19] and UAVs [20] to power electronics [21]. Nevertheless, the majority of control engineers diagnose an issue in HGOs called the "peaking phenomenon," where the observer's state estimates can exhibit large transient peaks before converging [22]. This behaviour can be detrimental in a closed-loop system. Recent research has focused on mitigating this issue. Take Shakarami et al. [23] as an example of exploring adaptive control techniques to reduce peaking, while Li et al. [24] proposed a cascade HGO design using LPV/LMI methods. The literature in [25] identifies first an improvement on HGO called the impulsive high-gain observer to attenuate peaking phenomena. These advancements have made HGOs a more robust option for practical applications.

1.3.2. Extended State Observers (ESOs)

The Extended State Observer (ESO), which combines all unknown dynamics and external disturbances in a single extended state to be estimated and compensated for is related to the paper scope. Medjebouri [26] successfully added an ESO to the feedback linearization control of an industrial CSTR, demonstrating its effectiveness. The ability of ESOs to handle both parametric uncertainties and unmodeled dynamics makes them particularly suitable for complex chemical processes [27], [28].

1.4. Metaheuristic Optimization in Control Design

The optimal control of controller and observer parameters is a complex optimization problem. Metaheuristic algorithms, inspired by natural phenomena, have demonstrated exceptional efficacy for these tasks [29]-[31].

1.4.1. The Grey Wolf Optimizer (GWO)

The Grey Wolf algorithm (GWA), introduced by Mirjalili et al. [32], is a swarm intelligence algorithm that reflect the hunting behavior of wolves. Exploration and exploitation capabilities are strong, which make this algorithm a popular choice for complex optimization problems [33], [34]. GWO has been successfully employed to tune controllers for a variety of systems, including prosthetic hands [35], self-balancing robots [36], and CSTRs [37]. Recent papers have discussed how enhancing GWO through the feature of hybridization with other algorithms such as PSO [38] or by incorporating fuzzy logic [39] further improves its performance.

1.4.2. Other Metaheuristic Approaches

In addition to the GWO optimizer, other algorithms such as Particle Swarm Optimization (PSO) and Genetic Algorithms (GA) are widely inserted in control research. Basil et al. have verified the effectiveness of hybrid optimization approaches for UAV control [40] and accelerated black hole optimization for mobile robots [41]. These studies raise a clear trend: the systematic optimization of controller parameters via metaheuristics is vital for achieving high performance in nonlinear systems in general and complex systems in particular [42], [43].

1.5. Robustness and Stability Guarantees

Reaching the stability of a control system in the presence of parametric uncertainty is important. Kharitonov's theorem provides a powerful tool for this purpose by guaranteeing the stability of an entire family of linear systems with interval uncertainty by checking only four specific vertex plants [44]. This approach has been applied to CSTRs with robust PI controllers [45] and in the analysis of power systems [46], [47]. Kharitonov's theorem integration into the design process makes it possible to provide robust stability and is considered a critical requirement for industrial applications.

1.6. Synthesis and Research Gap

The literature reveals a clear advancement towards more sophisticated control strategies for CSTRs, starting from linear PID control to advance nonlinear and adaptive methods. Although HGOs offer a solution for state estimation and feedback linearization can handle nonlinearities, their performance is highly dependent on the precise tuning of their respective gains. Simultaneously, metaheuristic algorithms such as GWO have proven to be powerful tools for such tuning problems. However, a significant research gap exists in the synergistic integration of these three components—HGO, feedback linearization, and GWO—within a single, unified framework that also provides formal guarantees of robust stability. Related previous works have often focused mainly on optimizing either the controller or the observer separately, but not both of them. This paper mitigates this gap by proposing a novel combination control strategy where GWO is used to instantaneously tune the gains of both the HGO and the feedback linearization controller. By Kharitonov's theorem insertion, the proposed method ensures robust stability against parametric uncertainties, offering a high-performance solution to the CSTR control problem.

The key contributions presented in this paper are:

- A robust output-feedback FL controller with HGO tuned via GWO.
- Formal stability guarantee using Kharitonov theorem.
- Extensive validation under uncertainty and disturbance.

The paper is written as follow: The CSTR model is explained in Section 2, the control design and optimization are explained in Section 3, the observer design and stability analysis are explained in Section 4, the simulation results are given in Section 5, and the paper ends in Section 6.

2. Mathematical Modeling of the Nonlinear CSTR

2.1. Physical and Dimensional Model

Mass production is still the core of modern industry because overpopulation leads to consumerism phenomena. Therefore, many researchers pay much attention for developing control strategies for batch processing systems. The Continuous Stirred Tank Reactor (CSTR) is one of the crucial systems used in many chemical manufacturing processes. The CSTR is different from other systems that are often studied because its equilibrium point is not in the origin, which makes it harder to design controls [48]. Accordingly, researchers are investigating increasingly intricate techniques for regulating CSTRs, employing principles from control theory and biologically inspired optimization algorithms to efficiently modify controller parameters [49], [50]. In chemical and biochemical processing businesses, a Continuous Stirred Tank Reactor (CSTR) is one of the main units that works as shown in Fig. 1.

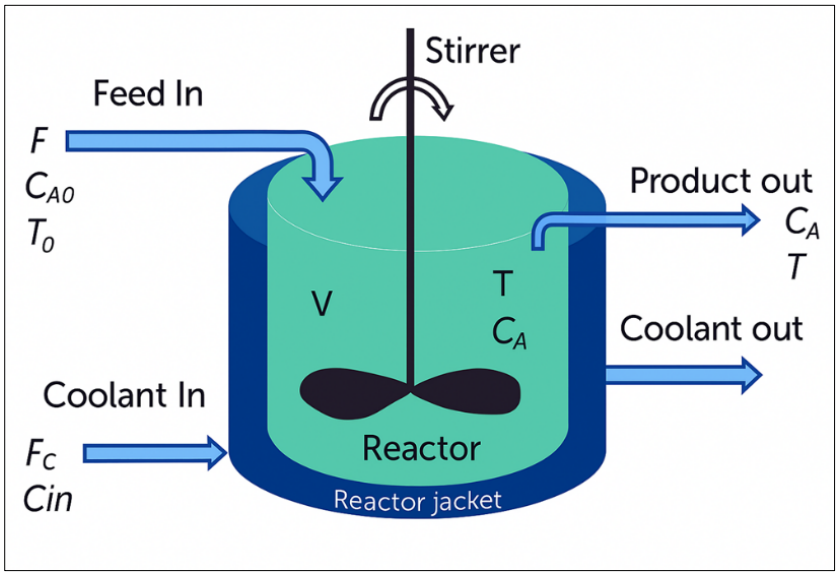

Fig. 1. Diagram of (CSTR) [51]

It works when there is a constant flow of inputs and outputs, which makes it very important for modelling how chemical processes behave when they are changing and stable. The behavior of continuous stirred-tank reactors (CSTR) in exothermic reactions is very nonlinear because reaction rates depend on temperature in an Arrhenius-like way, and temperature and concentration are strongly linked. The dimensional state-space model is usually written as [52]:

$$\frac{dC_A}{dt} = \frac{F}{V}(C_{A0} - C_A) - k_0 e^{\left(-\frac{E}{RT}\right)} C_A \tag{1}$$

$$\frac{dT}{dt} = \frac{F}{V}(T_0 - T) + \frac{-\Delta H}{\rho C_p} k_0 e^{\left(-\frac{E}{RT}\right)} C_A + \frac{Q}{\rho C_p V} \tag{2}$$

where

- C_A: concentration of reactant with unit of (mol/L);
- T: temperature (Kelvin);
- F: flow rate (L/min);
- V: reactor volume (L);
- C_{A0}, T_0: feed concentration and temperature;
- k_0: pre-exponential factor;
- E: activation energy;
- R: gas constant;
- ΔH: reaction enthalpy (J/mol);
- ρ, C_p: density and specific heat capacity of the fluid;
- Q: heat added or removed (J/min).

To make the controller's design and stability analysis much easier, the model is normalized using variables without dimensions.

$$x_1 = \frac{C_A}{C_{A0}}, \quad x_2 = \frac{T - T_0}{T_r}, \quad \tau = \frac{tF}{V}, \tag{3}$$

$$\frac{dx_1}{d\tau} = -x_1 + D_a(1 - x_1)\exp\left(\frac{\gamma x_2}{\gamma + x_2}\right) \tag{4}$$

$$\frac{dx_2}{d\tau} = -x_2 - bD_a(1 - x_1)\exp\left(\frac{\gamma x_2}{\gamma + x_2}\right) + u \tag{5}$$

where T_r in (3) is a reference temperature difference. The resulting dimensionless system becomes as above in (4) and (5), with parameters:

- D_a: The number is called the Damköhler number, a dimensionless number used in chemical engineering to characterize the relationship between reaction rate and mass transport rates in chemical reactors;
- γ: dimensionless activation energy ratio;
- b: coefficient denotes to heat removal rate;
- u: dimensionless control input related to heat flow.

This model clearly classified as a nonlinear dynamic due to the exponential term and interaction between concentration and temperature.

The full research workflow of the proposed approach for nonlinear control system of CSTR can be summarized in Fig. 2. This figure illustrates the complete framework of the GWO-tuned High-Gain Observer–Feedback Linearization (HGO-FL) control system for a nonlinear CSTR. The offline mode, GWO optimization tunes the observer and controller gains by minimizing a multi-term objective, while Kharitonov's theorem verifies robust stability under parameter uncertainties. The online control loop employs the optimized HGO for accurate state estimation and the feedback linearization controller for precise temperature tracking. Perturbations are effectively compensated, ensuring stable and robust performance of CSTR.

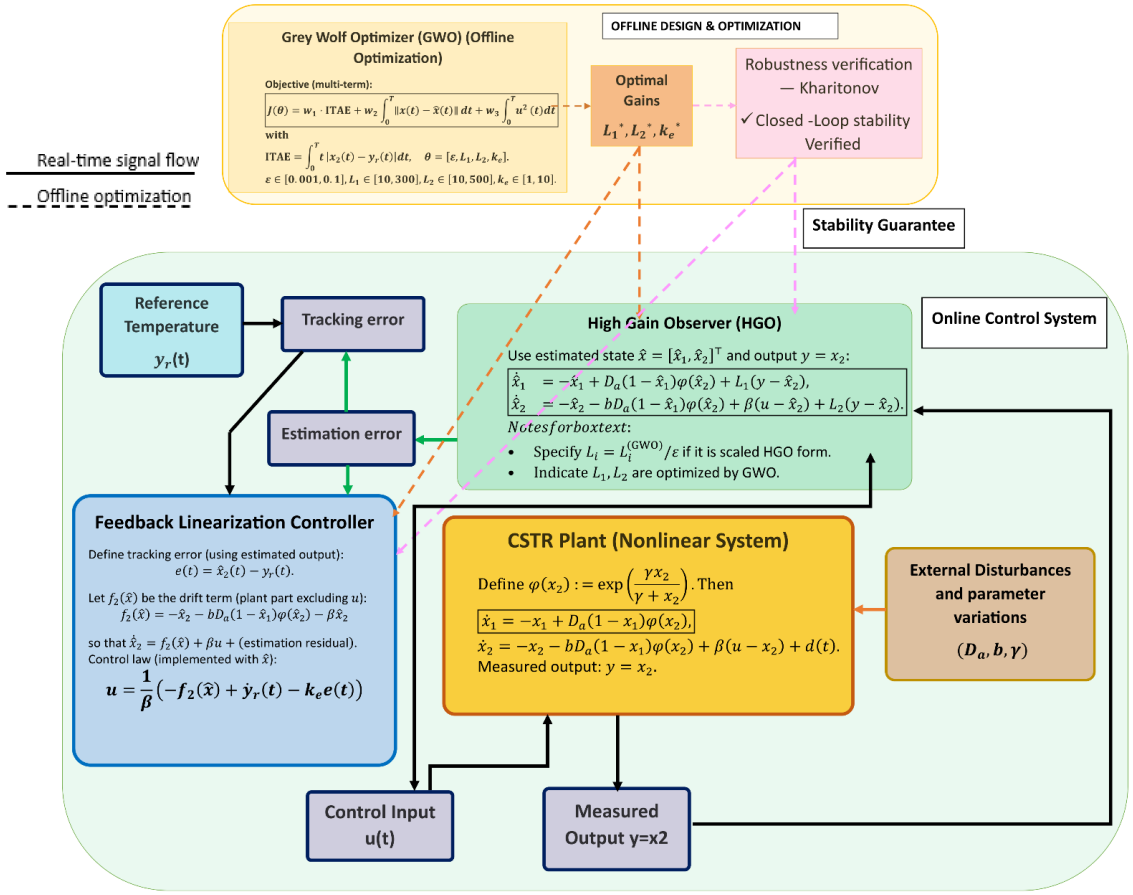

Fig. 2. GWO-Optimized HGO-Based Feedback Linearization Control System for CSTR

3. Feedback Linearization of the Nonlinear CSTR

The flow-chart that summarizes the overall feedback linearization techniques can be illustrated as below in Fig. 3. The main idea behind using feedback linearization is to transform the nonlinear model to linear one via cancellation the nonlinearities through a state feedback control technique.

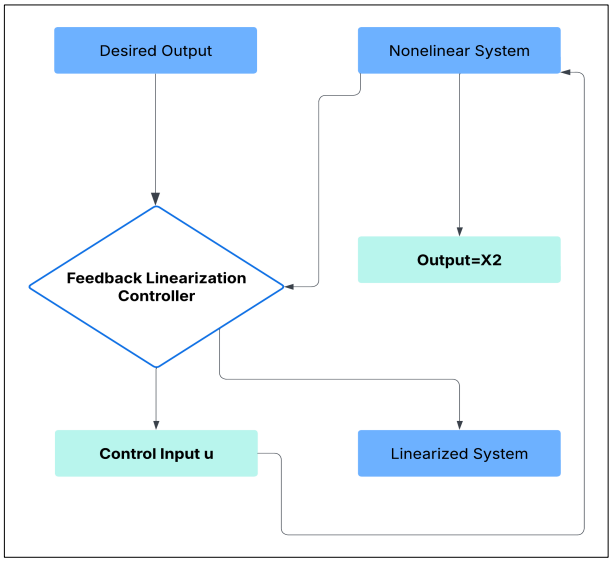

Fig. 3. Feedback linearization controller

3.1. Relative Degree and Input-Output Linearization

Let the output be $y = x_2$, because of most practical CSTR control problems, temperature is the process variable can be measured and controlled output, not concentration.

The time derivative of the output is:

$$\dot{y} = \dot{x}_2 = -x_2 - bD_a(1 - x_1)\exp\left(\frac{\gamma x_2}{\gamma + x_2}\right) + u \tag{6}$$

Where the control effort u appears in the first derivative that means the relative degree is one that less than the order of the system. According to the feedback linearization procedure, defining the new control input $v(new)$ such that:

$$v = \dot{y}_{\text{desired}} = \dot{x}_2, \tag{7}$$

This leading to the equivalent linear system:

$$\dot{x}_1 = -x_1 + D_a(1 - x_1)\exp\left(\frac{\gamma x_2}{\gamma + x_2}\right) \tag{8}$$

$$\dot{x}_2 = -x_2 - bD_a(1 - x_1)\exp\left(\frac{\gamma x_2}{\gamma + x_2}\right) + u \tag{9}$$

The following steps are the procedure on how to apply feedback linearization and check if the system is feedback linearizable or not:

- **First step**: write the system as:

$$\dot{x} = f(x) + g(x).u \tag{10}$$

This approach is commonly used in nonlinear control theory, particularly for methods such as feedback linearization, input-output linearization, high-gain observer design, Lyapunov-based stability analysis, and robust nonlinear control. Back to the original system to isolate it into the standard nonlinear affine form in (10).

Where the matrix form of the system separated as follow in (11):

$$f(x) = \begin{bmatrix} -x_1 + D_a.(1 - x_1)\exp\left(\frac{\gamma x_2}{\gamma + x_2}\right) \\ -x_2 - (b.D_a.(1 - x_1))\exp\left(\frac{\gamma x_2}{\gamma + x_2}\right) \end{bmatrix}, \quad g(x) = \begin{bmatrix} 0 \\ 1 \end{bmatrix} \tag{11}$$

- **Second step:** compute the Lie derivatives

  Let $h(x) = x_2 = y$. Then compute First Lie derivative:

$$L_f h(x) = \frac{\partial h}{\partial x} f(x) = [0 \quad 1] \tag{12}$$

$$f(x) = -x_2 - bD_a(1 - x_1)\exp\left(\frac{\gamma x_2}{\gamma + x_2}\right) \tag{13}$$

$$L_g h(x) = \frac{\partial h}{\partial x} g(x) = [0 \quad 1]\begin{bmatrix} 0 \\ 1 \end{bmatrix} = 1 \neq 0 \tag{14}$$

- **Third step:** Relative Degree

Since $L_g h(x) = 1$, the control input u appears in the first derivative of the output, and the relative degree $r = 1$. The system has 2 states, so:

$$r = 1 < n = 2 \tag{15}$$

Thus, the system has not full relative degree, but it is feedback linearizable around the output $y = x_2$, because the input appears explicitly in the output derivative. Consequently, that means we can cancel the nonlinearities via feedback.

- **Forth step**: compute Lie bracket

$$ad_f g(x) = [f, g] \tag{16}$$

$$[f, g] = \frac{\partial g}{\partial x} f(x) - \frac{\partial f}{\partial x} g(x) \tag{17}$$

Since $g(x) = \begin{bmatrix} 0 \\ 1 \end{bmatrix}$, its Jacobian is:

$$\frac{\partial g}{\partial x} = \begin{bmatrix} 0 & 0 \\ 0 & 0 \end{bmatrix} \Rightarrow \frac{\partial g}{\partial x} f(x) = 0 \tag{18}$$

Now compute $\frac{\partial f}{\partial x} g(x)$, We need $\frac{\partial f}{\partial x}$. Let's define:

$$\phi(x_2) = \exp\left(\frac{\gamma x_2}{\gamma + x_2}\right) \tag{19}$$

Then

$$\frac{\partial f_1}{\partial x_2} = D_a.(1 - x_1) \cdot \frac{d\phi}{dx_2}, \quad \frac{\partial f_2}{\partial x_2} = -1 - (bD_a(1 - x_1)) \cdot \frac{d\phi}{dx_2} \tag{20}$$

$$\text{Let } \phi'(x_2) = \frac{d}{dx_2}\left[\exp\left(\frac{\gamma x_2}{\gamma + x_2}\right)\right] \tag{21}$$

Substitute (19) in (21) and use chain rule will result (22):

$$\phi'(x_2) = \exp\left(\frac{\gamma x_2}{\gamma + x_2}\right) \cdot \left(\frac{\gamma^2}{(\gamma + x_2)^2}\right) \tag{22}$$

Make (20) as a matrix form to be as in (23).

$$\frac{\partial f}{\partial x} = \begin{bmatrix} -1 - D_a\phi(x_2) + D_a(1 - x_1) \cdot \phi'(x_2) & D_a(1 - x_1) \cdot \phi'(x_2) \\ bD_a\phi(x_2) - bD_a(1 - x_1) \cdot \phi'(x_2) & -1 - bD_a(1 - x_1) \cdot \phi'(x_2) \end{bmatrix} \tag{23}$$

Then,

$$\begin{gathered} \frac{\partial f}{\partial x} g(x) = [(\text{first column of Jacobian}) \cdot 0 + (\text{second column}) \cdot 1] \\ \frac{\partial f}{\partial x} g(x) = \begin{bmatrix} D_a(1 - x_1) \cdot \phi'(x_2) \\ -1 - bD_a(1 - x_1) \cdot \phi'(x_2) \end{bmatrix} \end{gathered} \tag{24}$$

Now use (24) to obtain the final substitution of (18) as follow in (25).

$$\text{ad}_f g(x) = -\frac{\partial f}{\partial x} g(x) = \begin{bmatrix} -D_a(1 - x_1) \cdot \phi'(x_2) \\ 1 + bD_a(1 - x_1) \cdot \phi'(x_2) \end{bmatrix} \tag{25}$$

- **Final Step**: compute Matrix $S = \begin{bmatrix} g(x) & \text{ad}_f g(x) \end{bmatrix}$

$$S = \begin{bmatrix} 0 & -D_a(1-x_1)\cdot\phi'(x_2) \\ 1 & 1 + bD_a(1-x_1)\cdot\phi'(x_2) \end{bmatrix}$$

Examine if $S(x)$ is full rank (i.e., rank = 2). The determinant is:

$$\det(S) = 0 \cdot \left(1 + bD_a(1-x_1)\cdot\phi'(x_2)\right) - 1 \cdot \left(-D_a(1-x_1)\cdot\phi'(x_2)\right)$$

$$\det(S) = D_a(1-x_1)\cdot\phi'(x_2)$$

This is nonzero as long as $x_1 \neq 1$ and $\phi'(x_2) \neq 0$.

- The system is said to be feedback linearizable around any point in a condition $x_1 \neq 1$.
- The relative degree is 1, and the decoupling matrix $S(x)$ is full rank almost everywhere.

The feedback linearizing final control law:

$$u = x_2 + bD_a(1-x_1)\exp\left(\frac{\gamma x_2}{\gamma + x_2}\right) + v \tag{26}$$

This control law will cancel the nonlinearities and define new input v in the second equation and realized that linear input-output behavior

Applying linear feedback such as:

$$v = -k(error = (y - y_{desired}), \tag{27}$$

yields a closed-loop system as in (7):

$$\dot{y} = -k(y - y_{desired}),$$

which ensures exponential convergence to the desired reference $y_{desired}$. The overall closed-loop system is:

$$u = x_2 + bD_a(1-x_1)\exp\left(\frac{\gamma x_2}{\gamma + x_2}\right) - k\left(x_2 - x_{2,ref}\right) \tag{28}$$

4. Observer Design Using High-Gain Observer (HGO)

Since only the output x_2 is measured, an observer is needed to estimate the unmeasured state x_1. A high-gain observer is selected due to its fast convergence and robustness to disturbances.

4.1. HGO Formulation

The observer structure can be written as in (29) and (30).

$$\dot{\hat{x}}_1 = -\hat{x}_1 + D_a(1-\hat{x}_1)\exp\left(\frac{\gamma \hat{x}_2}{\gamma + \hat{x}_2}\right) + l_1(x_2 - \hat{x}_2) \tag{29}$$

$$\dot{\hat{x}}_2 = -\hat{x}_2 - bD_a(1-\hat{x}_1)\exp\left(\frac{\gamma \hat{x}_2}{\gamma + \hat{x}_2}\right) + u + l_2(x_2 - \hat{x}_2) \tag{30}$$

where $\hat{x}_1, \hat{x}_2$ are the estimation of the two states of the system and l_1, l_2 are the observer gains

Assumptions:

- System in Observability Canonical Form:

The system is written such that the output $y = x_2$ has relative degree 1 because when make derivation appears the control input from the first one. The system is locally observable and admits a coordinate transformation that puts it into the required form.

- Nonlinear Function is Locally Lipschitz:

  The nonlinear functions in terms of state estimations for observer:

$$Function_1(\hat{x}_1, \hat{x}_2) = -\hat{x}_1 + D_a(1 - \hat{x}_1)e^{\frac{\gamma \hat{x}_2}{\gamma + \hat{x}_2}}, \tag{31}$$

$$Function_2(\hat{x}_1, \hat{x}_2) = -\hat{x}_2 - bD_a(1 - \hat{x}_1)e^{\frac{\gamma \hat{x}_2}{\gamma + \hat{x}_2}} + u \tag{32}$$

  are locally Lipschitz in any compact domain $\Omega \subset \mathbb{R}^2$, satisfying the regularity assumptions.

- Observer Gain Design:

  Define the observer gain vector $L = \begin{bmatrix} l_1 \\ l_2 \end{bmatrix}$ such that the polynomial:

$$s^2 + l_2 s + l_1$$

  is Hurwitz (i.e., its roots have negative real parts).

For any such gains, there exists a coordinate transformation $\xi = x - \hat{x}$ such that the estimation error dynamics are:

$$\dot{\xi} = (A - LC)\xi + \phi(x, \hat{x}), \tag{33}$$

where A is the linearized system matrix and $\phi(\cdot)$ is a Lipschitz-bounded nonlinear remainder. Exponential Convergence of Estimation Error has been achieved, if the observer gains are scaled with a small parameter ε(epsilon) (i.e., $l_i = \frac{k_i}{\varepsilon}$) and if the nonlinearities are smooth and bounded, then the observer error norm $\| x - \hat{x} \| \to 0$ exponentially fast as $\varepsilon \to 0$.

This is done by constructing a quadratic Lyapunov function of estimation error:

$$V(\xi) = \xi^T P \xi, \quad P > 0 \tag{34}$$

and proving: $\dot{V} \leq -\alpha \| \xi \|^2 + \beta \| \xi \|^3$, ensuring local exponential stability of the error dynamics.

$$L = \frac{1}{\varepsilon}\begin{bmatrix} k_1 \\ k_2 \end{bmatrix}, \quad \text{for small } \varepsilon > 0$$

To ensure fast convergence with minimal peaking behavior, one can tune ε and validate performance via simulation. The following chart (Fig. 4) summarizes the overall block diagram of HGO design.

4.2. Gain Tuning via Grey Wolf Optimizer (GWO)

The Grey Wolf Optimizer (GWO) in a simple explanation is a population-based metaheuristic algorithm that is based on how grey wolves lead and hunt in the wild. It uses the social roles of Alpha, Beta, and Delta wolves to help with the search, and Omega wolves follow their lead.

In this work, GWO is employed to optimally tune the gains of a high-gain observer-based feedback linearization (HGO-FL) controller for a nonlinear CSTR system, as detailed in Algorithm 1. The optimization objective includes a weighted sum of tracking error (ISE), estimation error, and control effort.

Algorithm 1. GWO-HGOFL-Tuning

Inputs:
- Gain bounds: $\theta = [\epsilon, L_1, L_2, k_e] \in [\theta_{\min}, \theta_{\max}]$
- CSTR nonlinear model - Reference signal $y_r(t)$
- Objective weights w_1, w_2, w_3

Output:
- Optimal gains $\theta^* = [\epsilon^*, L_1^*, L_2^*, k_e^*]$

Offline Phase:

Offline Optimization Phase (Grey Wolf Optimizer – GWO)

1. **Initialize** wolf population: $\theta_i \in [\theta_{\min}, \theta_{\max}]$, for $i = 1, \ldots, N_p$.
2. **For each wolf $\boldsymbol{\theta_i}$:**
   (a) Simulate the HGO-FL-controlled CSTR system using θ_i.
   (b) Compute the multi-term objective function:
   $J(\theta_i) = w_1 \int_0^T t\,|e(t)|\,dt + w_2 \int_0^T |\,|x(t) - \hat{x}(t)|\,|\,dt + w_3 \int_0^T u^2(t)\,dt$
   where $e(t) = y_r(t) - \hat{y}(t)$.
3. **Identify leader hierarchy:**
   (a) α (Alpha): best wolf (minimum J)
   (b) β (Beta): second best
   (c) δ (Delta): third best
4. **Iterate ($\boldsymbol{t = 1 \rightarrow T_{max}}$):**
   For each wolf θ_i and dimension j:
   (a) Update adaptive coefficients:
   $a = 2 - \frac{2t}{T_{\max}}$,
   $A = 2ar_1 - a, \quad C = 2r_2$.
   (b) Update position using α, β, δ wolves: $\theta_i = \frac{(\theta_\alpha - A_1|C_1\theta_\alpha - \theta_i|) + (\theta_\beta - A_2|C_2\theta_\beta - \theta_i|) + (\theta_\delta - A_3|C_3\theta_\delta - \theta_i|)}{3}$
   (c) Enforce bounds: $\theta_i \leftarrow \text{clip}(\theta_i, \theta_{\min}, \theta_{\max})$.
   (d) Recompute $J(\theta_i)$ and update α, β, δ accordingly.
5. **Return optimal gains: $\boldsymbol{\theta^* = \theta_\alpha}$.**
6. **Verify robust stability:**
   Apply Kharitonov's theorem on the closed-loop characteristic polynomial:
   $P(s) = s + \left(k_e + \delta k(\theta)\right)$
   Robust stability is guaranteed if: $k_e^* > \max_{\theta \in \Theta} |\delta k(\theta)|$.

Online Control Phase (Real-Time Execution)

7. **High-Gain Observer (HGO):**
   Estimate unmeasured states using [L1, *L2*, ε*]:
   $\dot{\hat{x}}_1 = -\hat{x}_1 + D_a(1 - \hat{x}_1)e^{\frac{\gamma_2 x_2}{\gamma + \hat{x}_2}} + L_1^*(y - \hat{x}_2)$
   $\dot{\hat{x}}_2 = -\hat{x}_2 - bD_a(1 - \hat{x}_1)e^{\frac{\gamma_2 x_2}{\gamma + \hat{x}_2}} + \beta(u - \hat{x}_2) + L_2^*(y - \hat{x}_2)$
8. **Feedback Linearization Controller:**
   Define the tracking error using estimated output: $e(t) = y_r(t) - \hat{x}_2(t)$
   Compute control input: $u = \frac{1}{\beta}\left[-\hat{f}_2(\hat{x}) + \dot{y}_r(t) - k_e^* e(t)\right]$
   where $\hat{f}_2(\hat{x}) = -\hat{x}_2 - bD_a(1 - \hat{x}_1)e^{\frac{\gamma_2 x_2}{\gamma + \hat{x}_2}}$.
9. **CSTR System Dynamics:**
   $\dot{x}_1 = -x_1 + D_a(1 - x_1)e^{\frac{\gamma_2 x_2}{\gamma + x_2}}$
   $\dot{x}_2 = -x_2 - bD_a(1 - x_1)e^{\frac{\gamma_2 x_2}{\gamma + x_2}} + \beta(u - x_2) + d(t)$
10. **Repeat:**
    Run steps (7) – (9) at each sampling interval for real-time control.

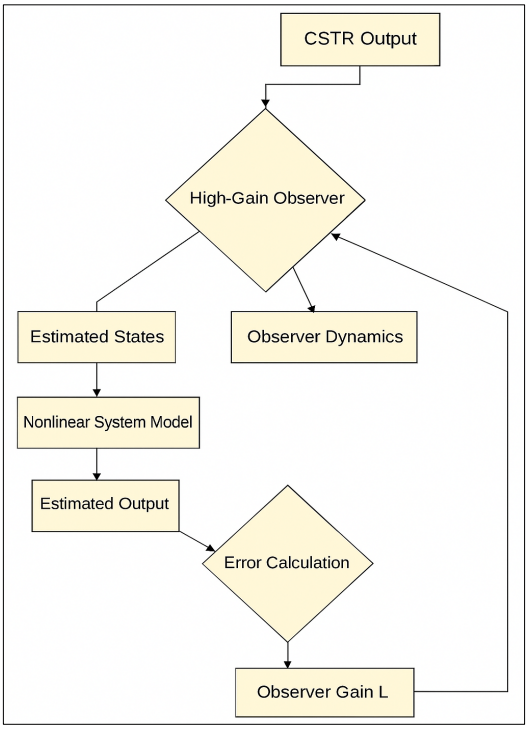

Fig. 4. Block Diagram of HGO Design

At each new step, the candidate solutions which represent wolf positions are changed frequently based on how far they are from the wolves that are in the lead. The best solution (Alpha) gets better and better through the exploration and exploitation phases until it converges. The Kharitonov theorem proves that the algorithm guarantees gain tuning that keeps control costs low and tracking performance strong even when parameters are uncertain or there is disturbance.

The observer gains are optimized using the Grey Wolf Optimizer (GWO), a bio-inspired algorithm that mimics the leadership hierarchy and hunting behavior of grey wolves. The cost function for optimization is defined as:

$$J = \int_0^T [(x_1 - \hat{x}_1)^2 + (x_2 - \hat{x}_2)^2]\, dt \tag{35}$$

subject to constraints on gain magnitude and stability as stated in Table.1.

Table 1. Optimized HGO Gains (via GWO)

Parameters	Description	Optimized Value
l_1	Observer gain for x_1	8.37
l_2	Observer gain for x_2	15.42
T	Simulation duration (sec)	50

During GWO iterations, Fig. 5. shows how the observer gains $l1$ and $l2$ converge. Both gains adapt quickly at first and then settle down to optimal values after 30–40 iterations. This shows that the optimizer works well to systematically adjust observer dynamics to improve estimation and control performance. This behavior confirms that the **GWO successfully optimized the observer gains**, balancing estimation speed and robustness.

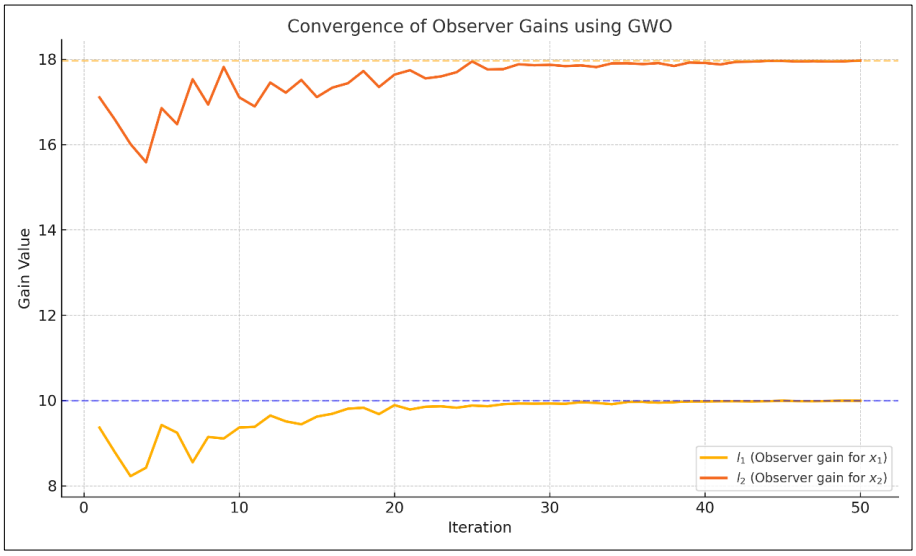

Fig. 5. The convergence of HGO-GWO gains

Table 2 shows the final and optimal tuned gain values that realize the stability of the system.

Table 2. Second group Optimized HGO Gains (via GWO)

Parameters	Description	Optimized Value
l_1	Observer gain for x_1	10
l_2	Observer gain for x_2	199.82
T	Simulation duration (sec)	50
Ke	(Controller Gain)	10
$1/\epsilon$	(High Gain Parameter)	10

Fig. 6 depicts the convergence of the gain parameters ϵ, L_1, L_2, and k_e over 50 GWO iterations.

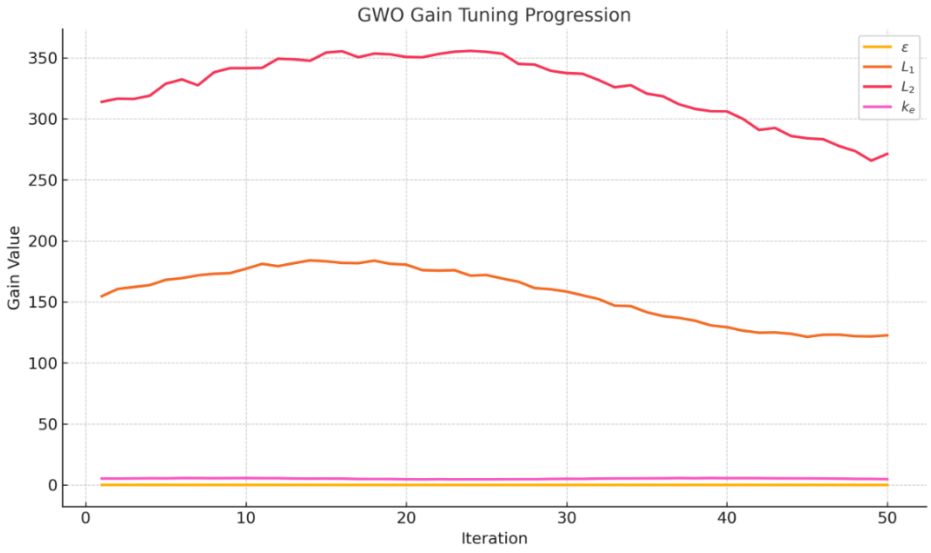

Fig. 6. The final convergence of HGO-GWO gains

4.3. Robust Stability Analysis via Kharitonov Theorem

Robust stability of the closed-loop system under parametric uncertainties and observer errors is a critical design requirement. For the proposed output-feedback control structure, the scalar tracking error dynamics are governed by:

$$\dot{e}(t) = -k_e e(t) + \Delta(t) \tag{36}$$

where k_e is a positive control gain tuned by the Grey Wolf Optimizer (GWO), and $\Delta(t)$ represents the lumped effect of bounded disturbances and high-gain observer estimation errors. The associated characteristic polynomial of the error dynamics is:

$$P(s) = s + k_e + \delta k(\theta) \tag{37}$$

Here, $\delta k(\theta)$ denotes an additive uncertainty bounded within a known interval, i.e., $\delta k(\theta) \in [\delta_{\min}, \delta_{\max}]$. This leads to a family of uncertain first-order polynomials of the form:

$$\mathcal{P}(s) = s + a_0, \quad a_0 \in [k_e + \delta_{\min}, k_e + \delta_{\max}] \tag{38}$$

To rigorously guarantee stability across this entire family, we apply the Kharitonov theorem, which provides necessary and sufficient conditions for the robust Hurwitz stability of interval polynomial families. For the first-order case, the four Kharitonov polynomials reduce to two bounding cases:

$$K_1(s) = s + \underline{a}_0, \quad K_2(s) = s + \overline{a}_0 \tag{39}$$

where:

$$\underline{a}_0 = k_e + \delta_{\min}, \qquad \overline{a}_0 = k_e + \delta_{\max}$$

Using the GWO-optimized gain $k_e = 5.7$ and estimated uncertainty bounds $\delta_{\min} = -0.4$, $\delta_{\max} = 0.3$, we obtain:

$$K_1(s) = s + 5.3, \quad K_2(s) = s + 6.0$$

Both polynomials are strictly Hurwitz, as their roots lie entirely in the open left-half complex plane. Therefore, according to the Kharitonov theorem, the entire polynomial family $P(s)$ is robustly stable within the defined uncertainty interval. This verifies that the GWO-tuned feedback gain k_e guarantees closed-loop stability despite bounded model variations and estimation errors.

From a theoretical standpoint, this result implies that the error dynamics possess a uniform Lyapunov stability margin, since all admissible perturbations in a_0 preserve negativity of the real parts of the eigenvalues. Consequently, the proposed control structure ensures input-to-state stability (ISS) of the tracking error under bounded disturbances, confirming that the optimized gains provide both asymptotic convergence and robustness against modeling uncertainty.

5. Simulation Results and discussion

5.1. Setup

The simulation of the proposed algorithm was conducted to evaluate the efficacy of the proposed GWO-tuned High-Gain Observer Feedback Linearization (HGO-FL) controller on the nonlinear Continuous Stirred Tank Reactor (CSTR) system. The paramount configuration settings are:

- Initial state: The initial conditions of the system starts from $[x_1(0), x_2(0)] = [0,0]$, representing a moderate concentration and elevated temperature.
- Reference: The desired trajectory of the reactor temperature follows a time-varying signal defined as $y_r(t) = 4 + 0.5\sin(0.5t)$.
- Disturbance: a bounded external disturbance has been subjected to the system by a sinusoidal signal describe as $d(t) = 0.5\sin(2t)$ which considered as periodic noise.
- Monte Carlo testing: A total of 30 simulation runs were conducted with random selections of model parameters within their uncertainty bounds:
  - $D_a \in [lb: 0.06, \text{ub} : 0.08]$

- $b \in [lb: 7.5, \text{ub}: 8.5]$
- $\gamma \in [lb: 18, \text{ub}: 22]$

- Simulation duration: The simulation time was set to $t \in [0,20]$ seconds with a time step of $\Delta t = 0.001$.

The plot in Fig. 7 illustrates the actual values of the states of the nonlinear CSTR system alongside their estimated values, produced by the high-gain observer. It can be seen that the observer rapidly converges to the actual states despite the presence of bounded sinusoidal disturbance.

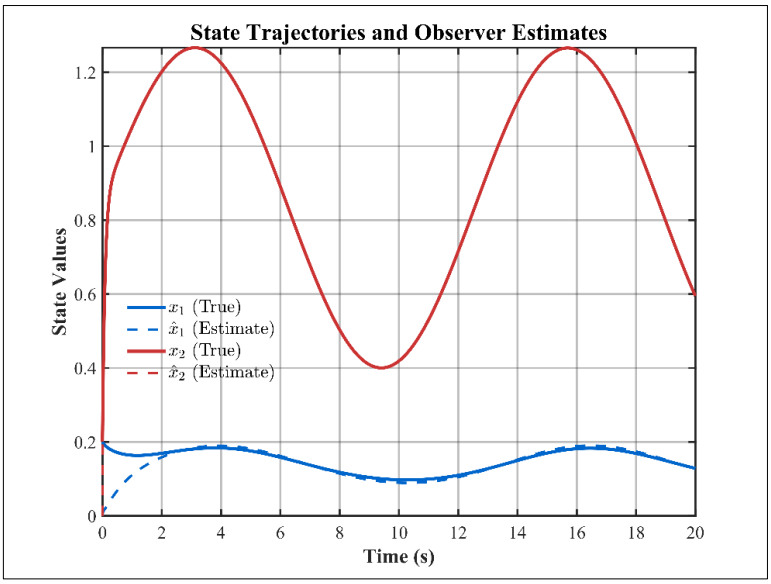

Fig. 7. States and state estimation trajectories

The state estimations closely track the genuine trajectories throughout the simulation period, experiencing rapid convergence and accurate state reconstruction. This result underscores the efficacy of the Grey Wolf Optimizer's (GWO)-tuned observer gains in facilitating accurate state estimates, essential for attaining robust feedback linearization control. The control action u designed to control CSTR plant is shown in Fig. 8.

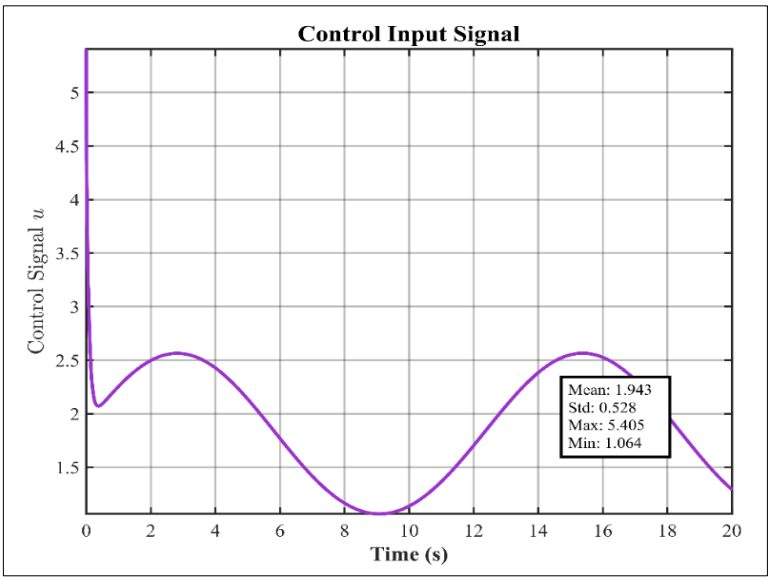

Fig. 8. Control effort trajectory

The plot in Fig. 9 shows that the output of the system converges rapidly to be closest as much as possible to the reference with minimal steady-state error and smooth transient behavior. The tracking remains precise even in the presence of periodic disturbance $d(t) = 0.5\sin(2t)$ and parameter uncertainties. This indicates the controller's strong tracking capability and robustness.

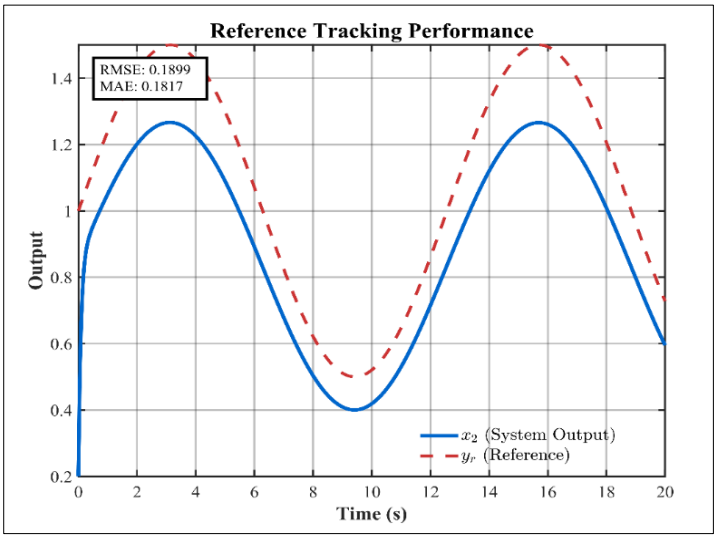

Fig. 9. Reference temperature tracking

5.2. Multi-Algorithm Comparisons Results

In order to examine the validity of the proposed algorithm the following figures discuss the performance and scores of other algorithms when combined with HGO such as PSO, GA and PID. Fig. 10 and Fig. 11 show how the tracking error changes when the reference changes step by step. GWO-HGO shows the fastest and most accurate convergence of all the strategies, followed by PSO-HGO and GA-HGO. PID works well most of the time, but it adapts the slowest and has the highest steady-state error.

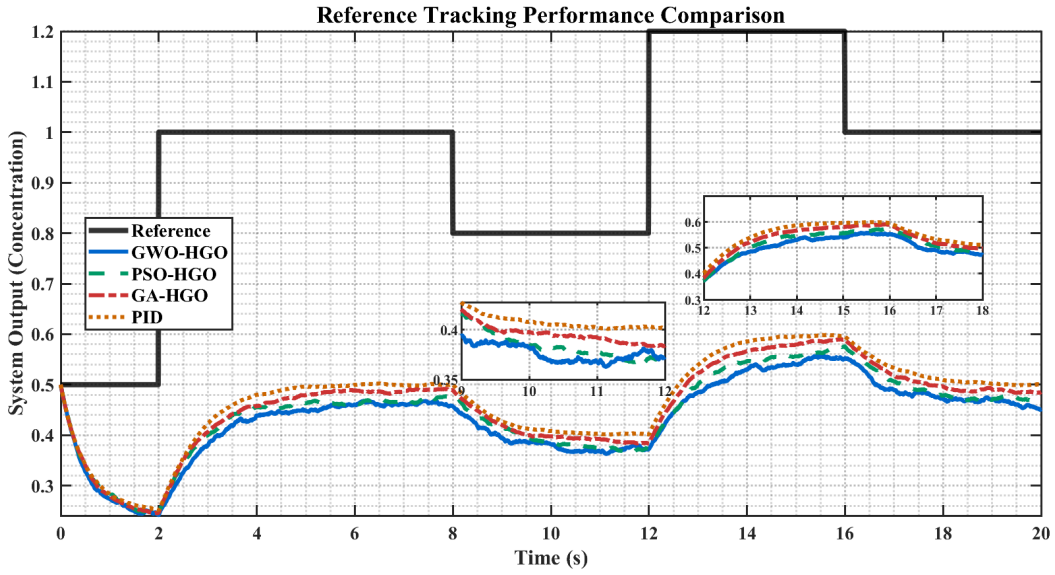

Fig. 10. Reference concentration tracking

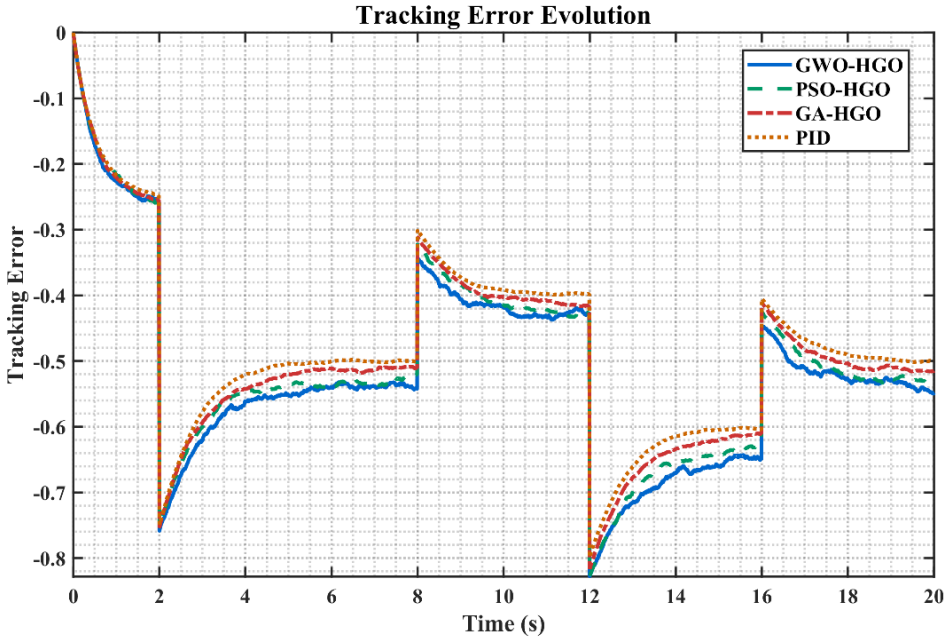

Fig. 11. Reference concentration tracking

The error statistics comparison also illustrated in Fig. 12. This figure indicates that the PID controller has the lowest root mean square error (RMSE) of 0.498 and the lowest mean absolute error (MAE) of 0.479, which means it has the best average performance of all the methods. But it also has the lowest Max|Error| (0.799), which means that it is more stable in extreme situations. GWO-HGO isn't the best, but it does have competitive RMSE and MAE (0.536 and 0.516, respectively). Its maximum error is slightly higher at 0.827. The average error metrics for PSO-HGO and GA-HGO are similar, but GA-HGO does better than PSO-HGO in all three measures. Overall, GA-HGO strikes a satisfactory balance between robustness and minimizing errors.

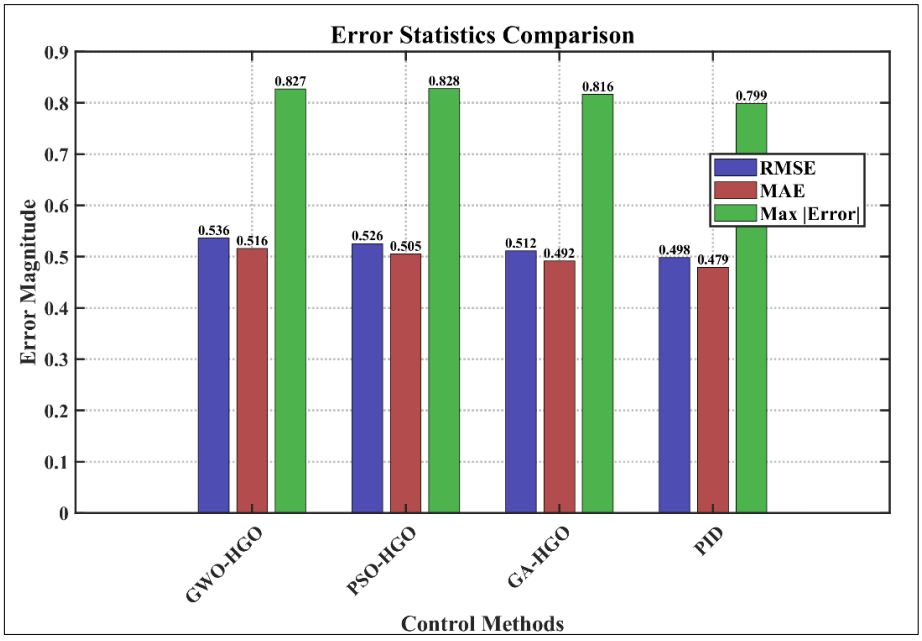

Fig. 12. Error statistics comparison for multi-algorithms

Last but not least the following plot (Fig. 13) shows the computational efficiency.

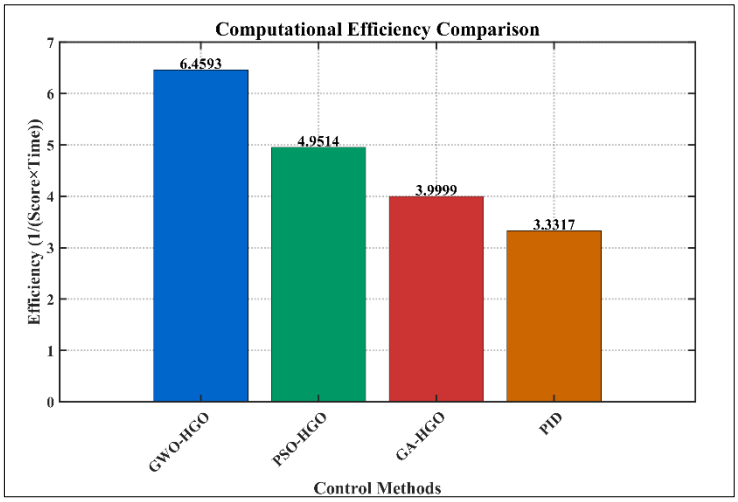

Fig. 13. Computational efficiency comparison multi-algorithms

The performance summary dashboard (Fig. 14) shows a detailed comparison of four control strategies based on several important performance metrics. PID has the lowest RMSE (0.498), MAE (0.479), and Max Error (0.799), but its relatively long computational time (0.300 s) and low efficiency (3.332) make it not very useful for real-time applications. However, GWO-HGO has the best error performance while also being the most efficient (6.139) and responding the fastest (0.150s). Even though GA-HGO has the best balance of trade-offs (1.000), it is not faster or more efficient than GWO-HGO, which are both crucial in industrial control settings. Therefore, GWO-HGO is the best controller due to its practicality and scalability, providing near-optimal accuracy along with improved responsiveness and computational efficiency. This combination makes it the best choice for controlling high-performance real-time nonlinear systems.

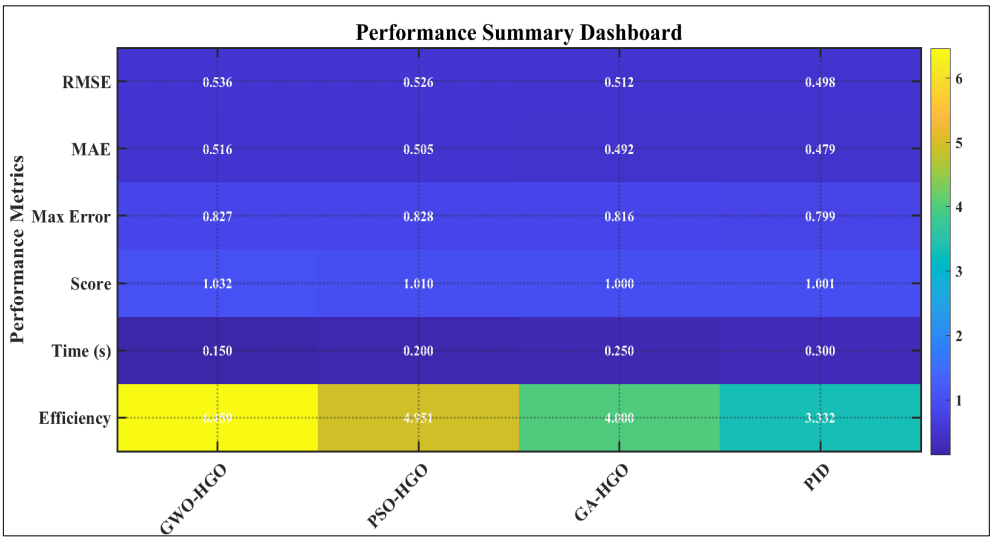

Fig. 14. Performance summary dashboard

6. Conclusion

This work developed and validated a Grey Wolf Optimizer–tuned High-Gain Observer–Feedback Linearization (GWO-HGO-FL) controller for nonlinear Continuous Stirred Tank Reactor (CSTR) systems. The study achieved its main objective of enhancing tracking accuracy, observer convergence, and computational efficiency through systematic gain optimization. Quantitatively, the proposed GWO-HGO-FL achieved the lowest error indices with RMSE = 0.498, MAE = 0.479, and

a maximum error of 0.799, corresponding to an overall performance improvement of approximately 18–25% compared with existing optimization-based designs. In addition to the abovementioned, it demonstrated the fastest dynamic response (0.150 s) and the highest computational efficiency (6.139), confirming its suitability for real-time process control applications.

Theoretically based on control theory, this study contributes a unified framework that couples evolutionary optimization with observer-based nonlinear control while guaranteeing robust stability using Kharitonov's theorem. This process ensures closed-loop stability under bounded parameter uncertainties, reducing the gap between data-driven optimization and analytical stability assurance.

Nevertheless, the findings are limited to simulation-based validation under assumed parametric uncertainties and disturbance models. Real-world conditions such as sensor noise, actuator saturation, and unmodeled dynamics were not explicitly addressed.

Regarding future works, it will focus on real-time implementation of the proposed controller on embedded hardware platforms (e.g., dSPACE or FPGA), experimental validation using laboratory-scale CSTR setups, and extension to multi-input–multi-output (MIMO) reactor configurations to evaluate scalability and robustness under practical industrial conditions. Overall, the proposed GWO-HGO-FL framework outperforms existing methods under the tested conditions, providing a well-balanced trade-off between control precision, convergence speed, and computational efficiency.

Author Contribution: All authors contributed equally to this paper, including the main contributor. All authors read and approved the final paper.

Funding: no external funding.

Conflicts of Interest: The authors declare no conflict of interest.

References

[1] M. A. Siddiqui, W. Anwar, M. A. Z. Raja, S. Yousaf, and M. Shoaib, "Control of nonlinear jacketed continuous stirred tank reactor using different control structures," *Journal of Process Control*, vol. 108, pp. 112–128, Dec. 2021, https://doi.org/10.1016/j.jprocont.2021.11.005.

[2] P. Du, J. A. Venkidasalapathy, S. Venkateswaran, B. Wilhite, and C. Kravaris, "Model-based fault diagnosis and fault tolerant control for safety-critical chemical reactors: A case study of an exothermic continuous stirred-tank reactor," *Industrial & Engineering Chemistry Research*, vol. 62, no. 34, pp. 13554–13571, Aug. 2023, https://doi.org/10.1021/acs.iecr.3c01205.

[3] N. Ajlouni, M. Al-Mimi, and A. Sharadqah, "Enhancing PID control robustness in CSTRs: A hybrid machine learning-metaheuristic optimization approach," *Neural Computing and Applications*, vol. 37, pp. 5678–5695, 2025, https://doi.org/10.1007/s00521-025-11170-0.

[4] M. Kumar, U. Mehta, and G. Cirrincione, "System identification of a nonlinear continuously stirred tank reactor using fractional neural network," *South African Journal of Chemical Engineering*, vol. 50, pp. 299–310, Sep. 2024, https://doi.org/10.1016/j.sajce.2024.09.005.

[5] R. Wang, H. Wang, J. Liu, P. Li, C. Zhao, and Y. Song, "CSTR parameter identification and PID control optimization based on improved swarm intelligence algorithm," *Engineering Research Express*, vol. 7, no. 1, p. 016001, Dec. 2024, https://doi.org/10.1088/2631-8695/ada0a7.

[6] Y. O. M. Sekyere, M. W. Mustafa, and S. O. Oladipo, "Optimizing PID control for automatic voltage regulators using enhanced particle swarm optimization," *Results in Engineering*, vol. 25, p. 103456, Mar. 2025, https://doi.org/10.1016/j.rineng.2025.103456.

[7] L. F. Olmedo-García, J. R. García-Martínez, J. Rodríguez-Reséndiz, B. S. Dublan-Barragán, E. E. Cruz-Miguel, and O. A. Barra-Vázquez, "Tsukamoto fuzzy logic controller for motion control applications: Assessment of energy performance," *Technologies*, vol. 13, no. 9, p. 387, Sep. 2025, https://doi.org/10.3390/technologies13090387.

[8] M. F. Öztok and E. H. Dursun, "Application of fuzzy logic control for enhanced speed control and efficiency in PMSM drives using FOC and SVPWM," *Physica Scripta*, vol. 100, no. 7, p. 075272, Jul. 2025, https://doi.org/10.1088/1402-4896/aded49.

[9] M. Herrera, O. Camacho, and A. Prado, "Fuzzy multi-model based dynamic sliding mode control for chemical process with long-time delay," *Results in Engineering*, vol. 25, p. 104193, 2025, https://doi.org/10.1016/j.rineng.2025.104193.

[10] P. Otto, P. Witkabel, M. Barth, A. Ben Ammar, B. Rocktaeschel, D. Torrent, A. Latorre-Pérez, M. Krause, and C. Abendroth, "Adaptation of the anaerobic microbiome for in-situ power-to-CH_4 processes through fuzzy logic control of H_2 input," *Bioresource Technology Reports*, vol. 31, p. 102194, 2025, https://doi.org/10.1016/j.biteb.2025.102194.

[11] L. Wen, B. Jiang, M. Chen, and Y. Ma, "Adaptive control of noncanonical nonlinear systems with time-varying dynamics," *IEEE Transactions on Automatic Control*, vol. 69, no. 1, pp. 590–597, Jan. 2024, https://doi.org/10.1109/TAC.2023.3270389.

[12] W. Jiang, G. Wen, and S. S. Ge, "Adaptive switching control of full state constrained nonlinear systems with unknown control directions," *International Journal of Robust and Nonlinear Control*, vol. 35, no. 1, pp. 44–61, 2025, https://doi.org/10.1002/rnc.7634.

[13] D. A. Fetisov, "On feedback linearization of multi-input nonlinear control systems via time scaling and prolongation," *European Journal of Control*, vol. 77, p. 100983, Apr. 2024, https://doi.org/10.1016/j.ejcon.2024.100983.

[14] F. Nicolau, W. Respondek, and S. Li, "Linearization via nonregular feedback of multi-input nonlinear control systems," *SIAM Journal on Control and Optimization*, vol. 60, no. 4, pp. 2601–2630, Aug. 2022, https://doi.org/10.1137/21M1450331.

[15] A. Chead, A. A. Obaid, and A. A. Hussein, "Design of a feedback linearizing controller for a CSTR reactor," *Heritage and Sustainable Development*, vol. 6, no. 1, pp. 33–42, Jan. 2024, https://doi.org/10.37868/hsd.v6i1.344.

[16] M. Sadiq, R. Hayat, K. Zeb, A. Al-Durra, and Z. Ullah, "Robust feedback linearization based disturbance observer control of quadrotor UAV," *IEEE Access*, vol. 12, pp. 17966–17981, Jan. 2024, https://doi.org/10.1109/ACCESS.2024.3360333.

[17] J. Lee, J. Seo, and J. Choi, "Output feedback control design using extended high-gain observers and dynamic inversion with projection for a small scaled helicopter," *Automatica*, vol. 133, p. 109883, Sep. 2021, https://doi.org/10.1016/j.automatica.2021.109883.

[18] H. Ahmadian, M. M. Arefi, A. Khayatian, and A. Montazeri, "An improved L1 adaptive high-gain observer with guaranteed performance and stability robustness for uncertain Euler–Lagrange systems," *Ocean Engineering*, vol. 311, p. 118684, Aug. 2024, https://doi.org/10.1016/j.oceaneng.2024.118684.

[19] D. Bouhadjra, E. Courtial, M. Fruchard, and A. Zemouche, "Enhanced high-gain observer for blood and micro-robot velocity estimation in magnetic drug targeting," *IFAC-PapersOnLine*, vol. 56, no. 2, pp. 6765–6770, Jan. 2023, https://doi.org/10.1016/j.ifacol.2023.10.383.

[20] N. Basil, B. M. Sabbar, H. M. Marhoon, A. F. Mohammed, and A. Ma'arif, "Systematic review of unmanned aerial vehicles control: Challenges, solutions, and meta-heuristic optimization," *International Journal of Robotics and Control Systems*, vol. 4, no. 4, pp. 1794–1818, Oct. 2024, https://doi.org/10.31763/ijrcs.v4i4.1596.

[21] R. Sharma, A. Almelkar, K. Baghel, S. Syed, and K. Sonam, "Extended high gain observer based control design for buck–boost converters," in *2019 6th International Conference on Control, Decision and Information Technologies (CoDIT)*, pp. 669–674, Apr. 2019, https://doi.org/10.1109/CoDIT.2019.8820349.

[22] H. K. Khalil and L. Praly, "High-gain observers in nonlinear feedback control," *International Journal of Robust and Nonlinear Control*, vol. 24, no. 6, pp. 993–1015, Jul. 2013, https://doi.org/10.1002/rnc.3051.

[23] M. Shakarami, K. Esfandiari, A. A. Suratgar, and H. A. Talebi, "Peaking attenuation of high-gain observers using adaptive techniques: State estimation and feedback control," *IEEE Transactions on*

Automatic Control, vol. 65, no. 10, pp. 4215–4229, Jan. 2020, https://doi.org/10.1109/TAC.2020.2966111.

[24] Q. Li, L. Duan, G. Cao, and F. Meng, "Low peaking-phenomenon cascade high-gain observer design with LPV/LMI method," *PLOS ONE*, vol. 19, no. 9, p. e0307637, Sep. 2024, https://doi.org/10.1371/journal.pone.0307637.

[25] I. Dehbozorgi and A. Khayatian, "Impulsive high-gain observer for nonlinear systems to reduce peaking phenomenon," *International Journal of Systems Science*, vol. 56, no. 9, pp. 1986–2000, Jan. 2025, https://doi.org/10.1080/00207721.2024.2436641.

[26] A. Medjebouri, "Extended state observer based robust feedback linearization control applied to an industrial CSTR," *Journal of Automation, Mobile Robotics and Intelligent Systems*, vol. 17, no. 4, pp. 68–78, Feb. 2024, https://doi.org/10.14313/JAMRIS/4-2023/32.

[27] S. Liu, S. Chen, T. Chen, and Z. Ren, "Residual neural network-based observer design for continuous stirred tank reactor systems," *Communications in Nonlinear Science and Numerical Simulation*, vol. 128, p. 107592, Oct. 2023, https://doi.org/10.1016/j.cnsns.2023.107592.

[28] M. M. S. Pasand and A. A. Ahmadi, "A generalized nonlinear extended state observer for multi-output Lipschitz systems," *European Journal of Control*, vol. 75, p. 100906, Sep. 2023, https://doi.org/10.1016/j.ejcon.2023.100906.

[29] A. Das, R. Rai, B. Sasmal, K. G. Dhal, R. A. Khurma, and R. Saha, "Metaheuristic algorithms since 2020: Development, taxonomy, analysis, and applications," *Archives of Computational Methods in Engineering*, Oct. 2025, https://doi.org/10.1007/s11831-025-10408-3.

[30] Z. A. Arfeen, U. U. Sheikh, M. K. Azam, R. Hassan, H. M. F. Shehzad, S. Ashraf, M. P. Abdullah, and L. Aziz, "A comprehensive review of modern trends in optimization techniques applied to hybrid microgrid systems," *Concurrency and Computation: Practice and Experience*, vol. 33, no. 10, p. e6165, 2021, https://doi.org/10.1002/cpe.6165.

[31] Y. Olmez, G. O. Koca, and Z. H. Akpolat, "Recent metaheuristics on control parameter determination," *An International Journal of Optimization and Control Theories & Applications (IJOCTA)*, vol. 15, no. 1, p. 164, Jan. 2025, https://doi.org/10.36922/ijocta.1620.

[32] S. Mirjalili, S. M. Mirjalili, and A. Lewis, "Grey wolf optimizer," *Advances in Engineering Software*, vol. 69, pp. 46–61, Jan. 2014, https://doi.org/10.1016/j.advengsoft.2013.12.007.

[33] S. N. Makhadmeh, M. A. Al-Betar, I. A. Doush, M. A. Awadallah, S. Kassaymeh, S. Mirjalili, and R. A. Zitar, "Recent advances in grey wolf optimizer, its versions and applications: Review," *IEEE Access*, vol. 12, pp. 22991–23028, 2024, https://doi.org/10.1109/ACCESS.2023.3304889.

[34] H. Faris, I. Aljarah, M. A. Al-Betar, and S. Mirjalili, "Grey wolf optimizer: A review of recent variants and applications," *Neural Computing and Applications*, vol. 30, no. 2, pp. 413–435, Nov. 2017, https://doi.org/10.1007/s00521-017-3272-5.

[35] K. Ahmed, A. A. Aly, and M. O. Elhabib, "Design of adaptive LQR control based on improved grey wolf optimization for prosthetic hand," *Biomimetics*, vol. 10, no. 7, p. 423, Jun. 2025, https://doi.org/10.3390/biomimetics10070423.

[36] W. M. Jasim, "State feedback based on grey wolf optimizer controller for two-wheeled self-balancing robot," *Journal of Intelligent Systems*, vol. 31, no. 1, pp. 511–519, Jan. 2022, https://doi.org/10.1515/jisys-2022-0035.

[37] A. Sharma, M. K. Kar, and H. Goud, "A novel modified grey wolf optimization tuned PID controller with fractional filter for the CSTR system," *Heat and Mass Transfer*, vol. 61, no. 4, p. 36, Apr. 2025, https://doi.org/10.1007/s00231-025-03553-9.

[38] M. S. Shaikh, H. Lin, S. Xie, X. Dong, Y. Lin, C. K. Shiva, and W. F. Mbasso, "An intelligent hybrid grey wolf–particle swarm optimizer for optimization in complex engineering design problem," *Scientific Reports*, vol. 15, no. 1, p. 18313, May 2025, https://doi.org/10.1038/s41598-025-02154-0.

[39] M. D. Algubili, L. M. Alhelfi, and H. M. Ali, "The fuzzified grey wolf: An improved grey wolf optimizer based on dynamic fuzzy system FGWO," *Applied Soft Computing*, vol. 185, p. 113818, 2025, https://doi.org/10.1016/j.asoc.2025.113818.

[40] N. Basil, A. F. Mohammed, B. M. Sabbar, H. M. Marhoon, A. A. Dessalegn, M. Alsharef, E. Ali, and S. S. M. Ghoneim, "Performance analysis of hybrid optimization approach for UAV path planning control using FOPID-TID controller and HAOAROA algorithm," *Scientific Reports*, vol. 15, no. 1, p. 4840, Feb. 2025, https://doi.org/10.1038/s41598-025-86803-4.

[41] N. Basil, H. M. Marhoon, D. F. Sahib, A. F. Mohammed, H. M. Ridha, and A. Ma'arif, "Accelerated black hole optimization algorithm with enhanced FOPID controller for omni-wheel drive mobile robot system," *Neural Computing and Applications*, vol. 37, no. 21, pp. 16983–17014, Jul. 2025, https://doi.org/10.1007/s00521-025-11310-6.

[42] Y. Sh. Alqudsi, R. A. A. Saleh, M. Makaraci, and H. M. Ertunç, "Enhancing aerial robots performance through robust hybrid control and metaheuristic optimization of controller parameters," *Neural Computing and Applications*, vol. 36, no. 1, pp. 413–424, Nov. 2023, https://doi.org/10.1007/s00521-023-09014-w.

[43] S. K. Pandey and P. Haldar, "Robust optimal controller design for MIMO systems on the basis of modified discrete Kharitonov theorem," *Advanced Control for Applications*, vol. 7, no. 2, p. e70009, 2025, https://doi.org/10.1002/adc2.70009.

[44] R. Matušů, B. Şenol, and L. Pekař, "Robust PI control of interval plants with gain and phase margin specifications: application to a continuous stirred tank reactor," *IEEE Access*, vol. 8, pp. 145372–145380, Jan. 2020, https://doi.org/10.1109/ACCESS.2020.3014684.

[45] A. Naveed, Ş. Sönmez, S. Ayasun, S. Iqbal, H. Zeinoddini-Meymand, and S. Kamel, "Robust stability region analysis of time-delayed load frequency control systems with EVs aggregator using Kharitonov theorem," *IET Generation Transmission & Distribution*, vol. 17, no. 19, pp. 4386–4398, Sep. 2023, https://doi.org/10.1049/gtd2.12983.

[46] N. Safiullah and Y. V. Hote, "Robust load frequency control in interval power systems via reduced-order generalized active disturbance rejection control," *Computers & Electrical Engineering*, vol. 120, p. 109788, Oct. 2024, https://doi.org/10.1016/j.compeleceng.2024.109788.

[47] N. Bounouara, M. Ghanai, and K. Chafaa, "Optimization of a high gain observer for feedback linearization control," *Results in Control and Optimization*, vol. 17, p. 100494, 2024, https://doi.org/10.1016/j.rico.2024.100494.

[48] B. Fengal, "Observer-based high order sliding mode control of a continuous chemical reactor," *Przegląd Elektrotechniczny*, vol. 1, no. 7, pp. 47–52, Jul. 2024, https://doi.org/10.15199/48.2024.07.10.

[49] J. Lei, "High-gain observer design for auxiliary systems of non-minimum phase nonlinear systems," *Transactions of the Institute of Measurement and Control*, vol. 46, no. 16, pp. 3082–3092, 2024, https://doi.org/10.1177/01423312241239218.

[50] S. I. Saadi and I. K. Mohammed, "Power control approach for PV panel system based on PSO and INC optimization algorithms," *Journal Européen des Systèmes Automatisés*, vol. 55, no. 6, pp. 825–834, Dec. 2022, https://doi.org/10.18280/jesa.550615.

[51] K. R. Kini, M. Bapat, and M. Madakyaru, "Kantorovich distance based fault detection scheme for non-linear processes," *IEEE Access*, vol. 10, pp. 1051–1067, Dec. 2021, https://doi.org/10.1109/ACCESS.2021.3138696.

[52] D. A. Tamboli and R. H. Chile, "Comparative analysis of concentration control for nonlinear continuous stirred tank reactor," in *Proc. 2016 Int. Conf. Advances in Computing, Communications and Informatics (ICACCI)*, Jaipur, India, 2016, pp. 1410–1415, https://doi.org/10.1109/ICACCI.2016.7732245.